

## THE ROLE OF PHYSICO-CHEMICAL PROPERTIES OF LIQUID SOLDER IN REACTIVE WETTING: THE Cu/SnZnIn SYSTEM

J. Pstruś<sup>a,\*</sup>

<sup>a</sup> Institute of Metallurgy and Materials Science, Polish Academy of Sciences, Krakow, Poland

(Received 28 July 2017; accepted 22 September 2017)

### Abstract

The measurements of surface tension, density and viscosity of liquid Sn-Zn eutectic alloys containing 0, 5, 10, 15 and 25 mole fraction of In were carried out using the sessile drop method, dilatometric technique and capillary method. The measurements were performed at temperature range between 493 and 843 K. The technique of sessile drop was applied in the measurements of wetting angles and spreading test in the SnZnIn/ Cu system.

Surface tension, density and viscosity measurements were carried out in a protective argon-hydrogen atmosphere. Wettability tests were performed in air in the presence of flux Alu33, at 250°C for 2 minutes. Subsequently, the microstructure of solder and the resulting joints was studied. The addition of In to eutectic Sn-Zn alloy improved the wetting properties and causes a reduction of thickness of the intermetallic compounds layer created at the interface between the liquid solder and the Cu substrate.

**Key words:** Lead-free solders; Sn-Zn-In liquid alloys; Intermetallic Cu-Zn; Wettability; Viscosity; Surface tension; Density.

### 1. Introduction

The continuous development of microelectronics in respect to miniaturization and efficiency improvement motivates the search for new materials and technologies capable of allowing on the one hand for cost reduction and for increasing of the density of connections and efficiency as well as for improving their reliability. The European Parliament's and the Council of Europe's directives issued in [1-3] 2003 and in 2008 prohibited the use of solders containing health detrimental metals such as lead and cadmium. Therefore for the past years an intense research has been conducted worldwide, the aim of which is to devise new alternatives for hazardous solders such as those containing lead. Soldering alloys based on Sn-Zn eutectic are competitive to commonly employed in electronics Sn-Ag, Sn-Ag-Cu based alloys with eutectic composition (SAC) due to the following [4-6]:

- lower melting temperatures (circa 198 °C whereas SAC melts above 220 °C)
- there is no forming of detrimental Vickers in with connections,
- better physic-chemical and mechanical properties (such as electric or plasticity),
- lower manufacturing costs, which are estimated to be 50% less as compared to the cost of SAC

production.

Sn-Zn alloys despite all the above mentioned advantages have much worse wetting properties as compared to SAC solders, and what is more they are prone to oxidation. Zhang et al. discussed in an overview the effect of alloying addition to Sn-Zn alloys [7]. Based on more than 100 references they list the most important alloying additions including: Bi, Cu, Ag, Al, In, Cr, Sb, Ni, Ge and Li. It was also showed that using several alloying additives, a significant improvement in solder properties can be achieved [7].

On the one hand additions are expected to improve the oxidation resistance (Al) and on the other hand wetting ability (Cu, Li) as well as to increase spreading velocity (Li) (author's own unpublished research). Research literature suggests a positive effect of indium on the wettability, melting point and mechanical properties [8-13]. Low melting point solders are particularly used in microelectronics for thermally degrading components such as circuit board laminates, integrated circuit (IC) package encapsulates and heat sensitive devices [8]. McCormack et al. [10] noted that the addition to the eutectic Sn-Zn alloy 5% or 10% indium reduced the melting point to 188 °C or 178 °C respectively. They performed a preliminary measurement of the

*Dedicated to the memory of Professor Dragana Živković*

\* Corresponding author: j.pstrus@imim.pl



wettability by solderability tester in air, in the presence of a flux, showing that the Sn-15Zn-6In alloys may have comparable properties to that obtained for eutectic Sn-Zn and Sn-Pb alloys.

A number of studies were conducted on the effect of the indium addition on the properties of Sn-Ag and Sn-Ag-Cu eutectic alloys [13-17]. Sebo et al. [14] showed that for Sn-Ag liquid eutectic alloys with increasing indium content the contact angle decreases while the surface tension does not change. The same correlation noted by Takemoto [15] in the wetting balance test where the contact angle decreases while the interfacial tension does not change. Therefore, one of the tasks covered by this article is to answer the question whether the addition of indium to the eutectic Sn-Zn alloy will produce a similar effect.

Interest in alloys based on Sn-Zn eutectic as a lead-free solder is enormous. Almost all of the existing scientific articles are related to corrosion studies [18-21], to thermodynamic description [22-25], the influence of alloying additives on melting points, wetting, mechanical and electrical properties [26-28] and on properties solder joints [29-32]. However, there is no report in the literature that describe the effect of physicochemical properties of these alloys on the wettability and on the phenomena occurring in the solder joint.

This article shows these liquid solder properties such as surface tension, density and viscosity with wettability and microstructure of solder joints.

## 2. Experimental

The studied alloys were prepared by melting pure metals (Sn: 99.999%, Zn: 99.95%, and In: 99.999%) in graphite crucibles, in a glovebox filled with Ar

(99.9992%) protective atmosphere (oxygen and water vapor pressure less than 1 ppm) to avoid oxidation. Measurements of the surface tension of liquid alloys have been conducted using the method of sessile drop (SD). For surface tension, a new setup (Fig. 1) was built. It consists of a vertical furnace, control module, and module collecting and archiving the data. A sample of the solder (1) with a diameter of 7.5 mm and a height of approx. 8 mm, was degreased in ethanol and ammonia after mechanical cleaning and then placed in a graphite crucible (Fig. 1b). The height of the roller of the test alloy was chosen so that after melting, the weight of the droplet was about 1.5 g. Graphite crucible with the metal under test were placed in a hollow molybdenum cone that was suspended on a molybdenum thread attached to the micrometer screw (7) in the furnace cover (5). The whole was in the quartz tube (2) to which the closing flanges (5) were attached. After loading the sample, the air was pumped from the system and the system was flushed with purified gas (Ar-15% $H_2$ ). Upon reaching the first measurement temperature, the sample was heated for about 10min, then were taken 5 photographs by the digital camera (3). Then, using a screw (7), the sample was rotated by 180° and was taken another 5 photographs. Due to strong zinc evaporation, one sample of solder was used to measure only at temperature. Temperature fluctuations were about 1°C. Due to the use of molybdenum thread with molybdenum cone, the drop of liquid solder was always vertically. For determination of surface tension from the form of a sessile drop, Dorsey equation was used [33].

Wetting tests were carried out on copper pads (99.95%) [34]. Copper pads were prepared in accordance with EN ISO 9455-10:2000. Mass of each

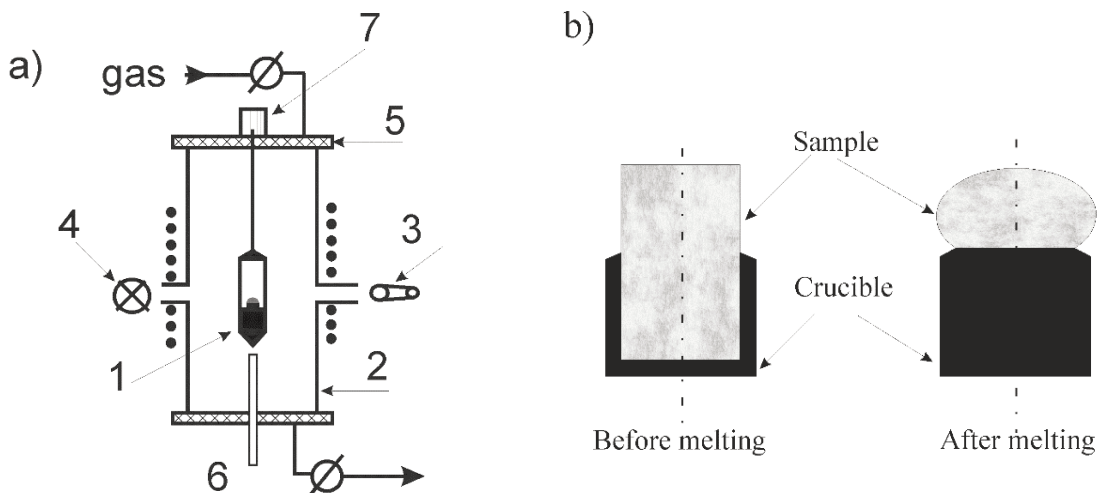


**Figure 1.** a) Scheme of new equipment for measuring surface tension by the method of "sessile drop" 1 – molybdenum "vertical" with crucible and sample, 2 – quartz tube with sight glass, 3 – digital camera, 4 – lighting, 5 – closing flanges, 6 – thermocouple, 7 – micrometer screw with molybdenum thread, b) Sample of the tested alloy together with the crucible.

sample used for spreading tests was 0.5 g, and the dimensions of the copper pads were 40 x 40 x 2.5 mm. Wetting tests were performed at 523 K, by means of flux ALU33; the wetting time was 2 min. After wetting tests, the flux residue was washed out with tap water. The area of spreading was calculated using the open software “ImageJ”. The microstructural and EDS analyses were performed using FEI Quanta 3D FEG system, at 20 kV and WD 10 mm, by means of the standard less Analysis EDAX Pegasus XM4i software.

The capillary method was used for measuring of viscosity of the Sn-Zn-In liquid alloys [35].

Density of liquid alloys has been conducted using the dilatometric method [36, 37].

### 3. Results

The measurements of surface tension, density and viscosity of liquid Sn-Zn-In alloys were carried out for 5 alloys of the following concentrations (mole fraction): Sn-14Zn, Sn-14Zn+5In, Sn-14Zn+10In, Sn-14Zn+15In, Sn-14Zn+25In, at temperatures from 493 K up to 823 K. Measurements of the wetting angles and spreading tests of Sn-Zn-In liquid alloys on Cu substrates were performed at 523 K after a 2 min heating.

#### 3.1 Properties of liquid solders

##### 3.1.1 Thermodynamics

Using “Pandat” package and thermodynamic data [23, 24 and 39] the phase diagram has been calculated and shown in Fig. 2 The research work of the authors [22, 23] show, that addition of indium in the Sn-Zn eutectic alloys decrease the melting point to about 178°C, as well as reducing the clotting range of ternary alloys, but simultaneously introducing the

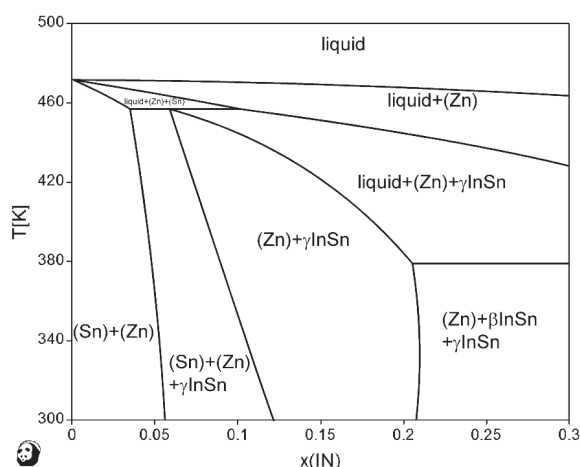


Figure 2. Sn-Zn<sub>eut</sub>+In pseudo-binary phase diagram (thermodynamic data of [23,24 and 38])

unfavorable  $\gamma$ -InSn phase. Therefore, it suggests that in the case of solder alloys, the addition of indium should not be greater than 5at%. From the phase diagram shown in Figure 2, it is clear that increasing the indium content decreases the melting point and extends the solidification range. It also causes the appearance of phases: first hexagonal gamma, later tetragonal beta. As further demonstrated in the case of solder alloys it may be beneficial. The Sn-20In-2.8Ag alloy with a melting range of 178-189 °C is often used as a solder for bonding at the BGA technology [39-41]. It only consists of  $\gamma$  phase, which is a relatively hard phase.

##### 3.1.2 Density

The results of density measurements for Sn-14Zn+In liquid alloys are presented in the form of straight-line temperature dependencies in Table 1 and in Figs. 3 and 4, together with literature data [42-45]. The density for all compositions decreases with increasing temperature. The measured density values of liquid Sn-Zn eutectic alloy are in good agreement with the literature data. Densities of pure indium, tin and zinc were presented in earlier papers [46, 47] was used in this work to calculate molar volume of In-Sn-Zn alloys. Using the formula (1), based on the obtained density equations, the molar volume of alloys was calculated and its isotherms are presented in Figure 5.

$$V_{i,j,k} = \frac{X_i M_i + X_j M_j + X_k M_k}{\rho_{ijk}} \quad (1)$$

Where:  $M_i, M_j, M_k$  – molar masses;  $X_i, X_j, X_k$  – molar fractions of components i – Sn, j – Zn, k – In;  $\rho_{ijk}$  - density of alloys.

The positive deviations of molar volume from the ideal course for all temperatures (Fig.5). At lower temperatures, this deviation is higher and decreases with increasing temperature. The Sn-Zn-In liquid alloys have excess volume during the solution formation, so it can be presumed that their thermodynamic properties are rather determined by changing the molar volume at their formation rather than by their structure and interactions atoms. [48].

Table 1. The results of measurements of density of liquid Sn-14Zn+In alloys, together with the estimated errors of coefficients A and B and calculated density  $\rho$  at 523 K.

$X_{In}$	$\rho=A+B \cdot T$ $g \cdot cm^{-3}$	$\rho$ (523K) $g \cdot cm^{-3}$	Err (A) $g \cdot cm^{-3}$	Err (B) $g \cdot cm^{-3} \cdot K^{-1}$
0	7.2655-0.000646	6.928±0.028	±0.075	±0.000118
0.05	7.2643-0.000682	6.908±0.012	±0.033	±0.000052
0.1	7.1238-0.000477	6.874±0.026	±0.070	±0.000111
0.15	7.1741-0.000577	6.872±0.011	±0.029	±0.000045
0.25	7.2684-0.000654	6.926±0.014	±0.039	±0.000061



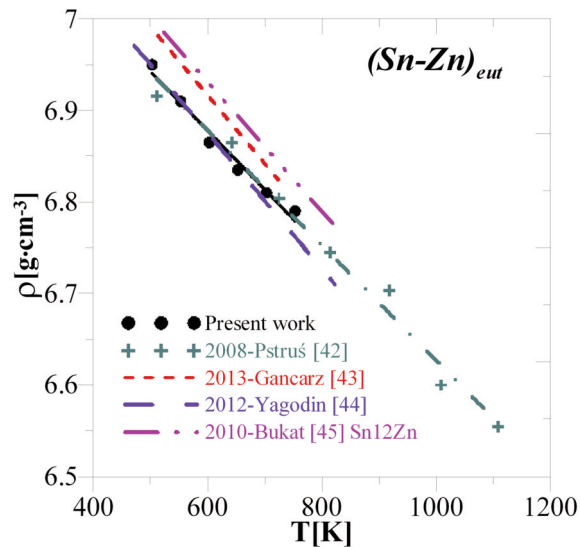


Figure 3. Comparison of temperature dependence of density for Sn-Zn eutectic alloy measured in present work by the dilatometric method and those from the literature [42-45].

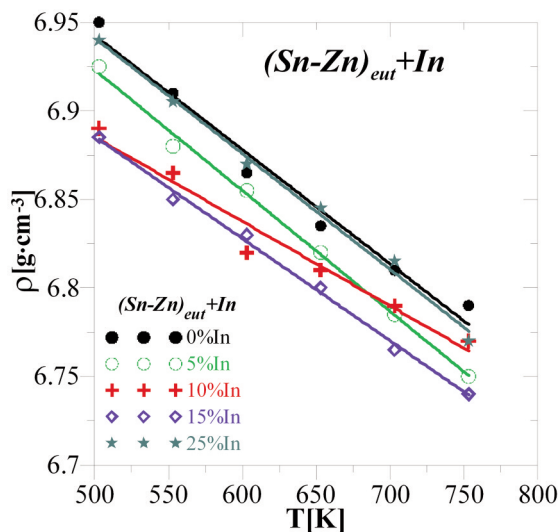


Figure 4. Temperature dependence of density for Sn-Zn-In alloys.

Based on the equations of density alloys in Table 1 and the density of the pure metals [46, 47] molar volume change during formation of the solution was calculated by the formula (2) and shown in Figure 6.

$$\Delta V_M^{Ex} = \frac{x_i M_i + x_j M_j + x_k M_k}{\rho_{ijk}} - \frac{x_i M_i}{\rho_i} - \frac{x_j M_j}{\rho_j} - \frac{x_k M_k}{\rho_k} \quad (2)$$

where:  $M_i$ ,  $M_j$ ,  $M_k$  – molar masses,  $X_i$ ,  $X_j$ ,  $X_k$  – molar fractions of components  $i$ ,  $j$ ,  $k$ ;

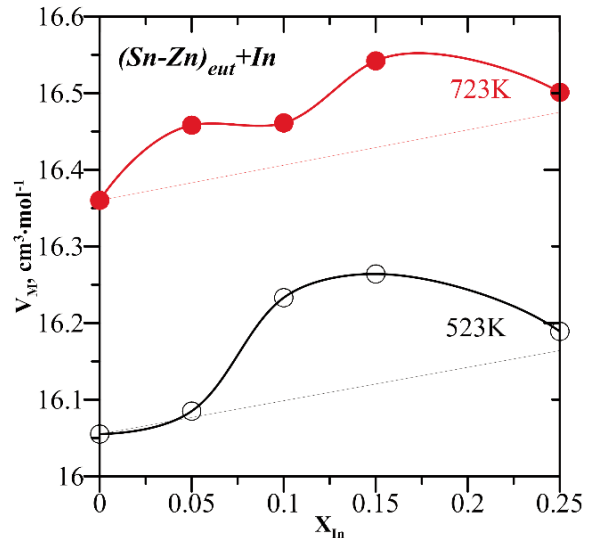


Figure 5. Isotherms of molar volume for  $(Sn-Zn)_{eut} + In$  liquid alloys.

$\rho_{ijk}$  – density of alloys;  $\rho_i$ ,  $\rho_j$ ,  $\rho_k$  – density of pure liquid metals.

As shown in Figure 6 and the phase diagram 1, the existence of an excess molar volume of liquid alloys correlates fairly well with the presence of phase  $\gamma$ .

Furthermore, it can be seen that the extent of this excess decreases with increasing temperature. However, on the other hand, the deviation of the molar volume from additivity does not exceed 2% and oscillates around a density measurement error of about 1%.

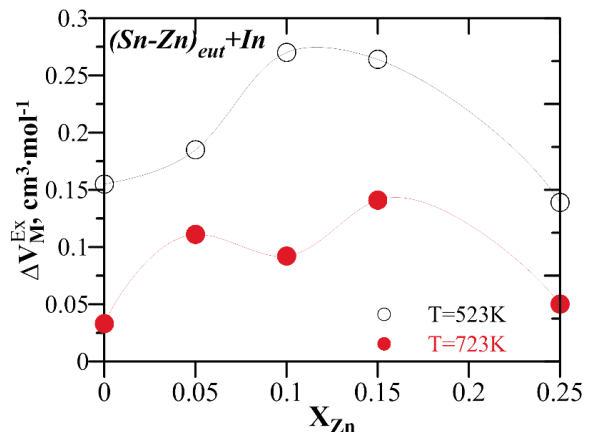


Figure 6. The excess molar volume  $\Delta V_M^{Ex}$  of  $(Sn-Zn)_{eut} + In$  liquid alloys.

### 3.1.3 Surface Tension

Linear dependence on the surface tension  $\sigma = A + BT$  of temperature is shown in Figs. 7 and 8 and are presented along with estimated errors of the coefficients in Table 2. Surface tension for all



compositions decreases with increasing temperature.

Fig. 6 shows a comparison of data of the surface tension of the Sn-Zn eutectic alloy measured in present work by the sessile drop (s.d.) method and those from the literature [42, 45] – maximum bubble (m.b.) pressure method, [43] – discharge crucible (d.c.) method.

The highest surface tension values were obtained using the method “d.c.” the lowest values by method “s.d.” Differences in the results obtained by these methods are about 5%. While the surface tension values of these alloys obtained using the “m.b.” method were about 2% higher than presented in this article. A similar tendency has been observed during the measurements of the surface tension of pure metals Sn, Zn and In and the Sn-In alloys [47]. Always the surface tension values measured with the „m.b.” method are higher than these received with the „s.d.” method.

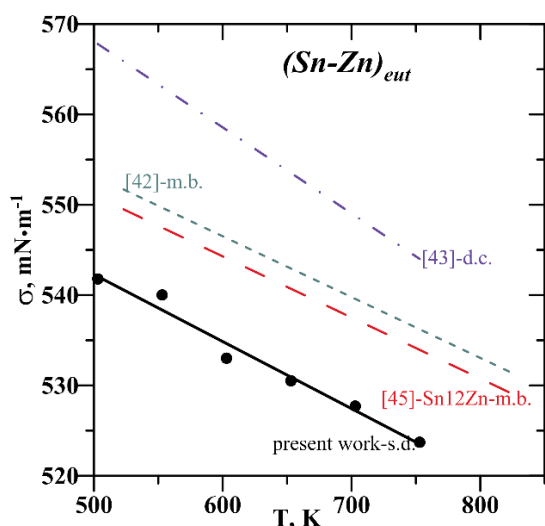


Figure 7. Comparison of temperature dependence of surface tension for Sn-Zn eutectic alloy measured in present work by the sessile drop method and those from the literature: [42, 45] – maximum bubble (m.b.) pressure method, [43] – discharge crucible (d.c.) method.

Table 2. The results of measurements of surface tension of liquid Sn-14Zn+In alloys, together with the estimated errors of coefficients A and B and calculated density  $\rho$  at 523 K.

$X_{In}$	$\sigma=A+B \cdot T$ mN·m <sup>-1</sup>	$\sigma$ (523K) mN·m <sup>-1</sup>	Err(A) mN·m <sup>-1</sup>	Err(B) mN·m <sup>-1</sup> ·K <sup>-1</sup>
0	579.4 -0.0742	540.6±3.3	±9.0	±0.0142
0.05	572.5 -0.0653	538.4±5.1	±13.8	±0.0217
0.1	577.3 -0.0671	542.2±2.9	±7.8	±0.0124
0.15	563.8 -0.0479	538.8±2.5	±6.7	±0.0106
0.25	573.4 -0.0594	542.3±3.9	±10.7	±0.0168

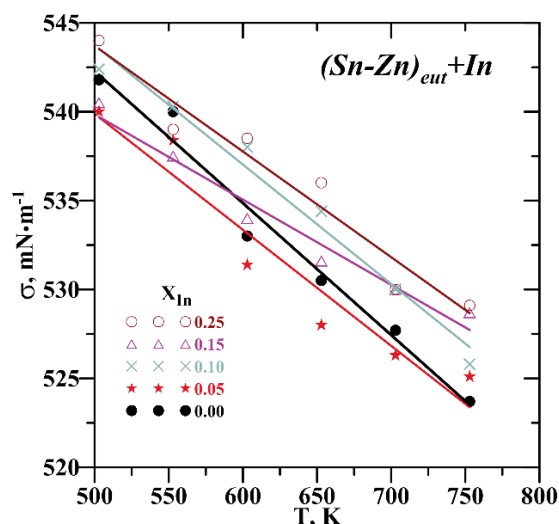


Figure 8. Temperature dependence of surface tension for (Sn-Zn)<sub>eut</sub>+In liquid alloys.

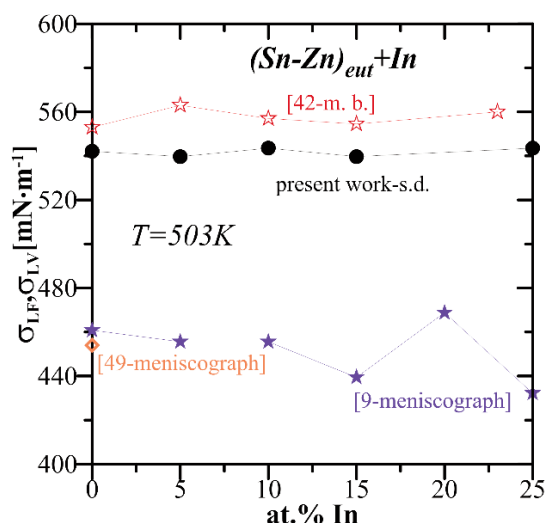


Figure 9. Comparison of surface tension ( $\sigma_{LV}$ ) isotherms and interfacial tension ( $\sigma_{LF}$ ) isotherms vs. concentration of indium for (Sn-Zn)<sub>eut</sub>+In alloys measured in present work by the sessile drop method and those from the literature [9, 49] – meniscograph, [42] – maximum bubble pressure.

Fig. 9 shows the surface tension isotherms of Sn-Zn-In alloys vs indium composition, obtained in two methods: m.b. [42] and s.d. as compared to isotherms of interfacial tension calculated from the meniscus method [9, 49]. Figure 9 shows that the addition of indium to the Sn-Zn eutectic did not change both the surface tension as  $\sigma_{LV}$  and the interfacial  $\sigma_{LF}$ . Also, there is a relationship between surface tension and interfacial tension. When the surface tension decreases with the change in composition, also the interfacial tension decreases.



### 3.1.4 Viscosity

The capillary method was used in the measurements of the viscosity  $\eta$  of the Sn-Zn-In liquid alloys. This capillary method has been described in earlier papers [35, 50]. Results of viscosity measurements as a function of temperature are plotted in Fig. 10 for Sn-Zn eutectic alloy and in Fig. 11 for Sn - Zn + In alloys. The decrease of viscosity with increasing temperature can be interpreted by Arrhenius empirical equation (3), and the results are shown in Table 3.

$$\eta = Ae^{\left(\frac{E}{RT}\right)} \quad (3)$$

Where: A is the constant (mPa·s), R is the gas constant ( $\text{J}\cdot\text{mol}^{-1}\cdot\text{K}^{-1}$ ), E is the flow activation energy ( $\text{J}\cdot\text{mol}^{-1}$ ).

Figure 12 shows isotherms of viscosity at temperatures of 523 and 723K. They were calculated on the basis of equation (3) and of parameters of the

**Table 3.** Fitting parameters of the Arrhenius equation to the viscosity for Sn-Zn eutectic alloy and for Sn - Zn + In alloys.

Alloy	A, mPa·s	$E_v$ , $\text{J}\cdot\text{mol}^{-1}$	References
Sn-Zn eutectic	0.355	7.855	[43]
Sn-Zn eutectic	0.364	7.762	[51]
Sn-Zn eutectic	0.466	5.58	[52]
Sn-Zn eutectic	0.445	5.873	[53]
Sn-Zn eutectic	0.441	6.231	This study
Sn-Zn eutectic+5%In	0.435	6.582	This study
Sn-Zn eutectic+10%In	0.44	7.256	This study
Sn-Zn eutectic+15%In	0.487	6.381	This study
Sn-Zn eutectic+25%In	0.377	7.232	This study

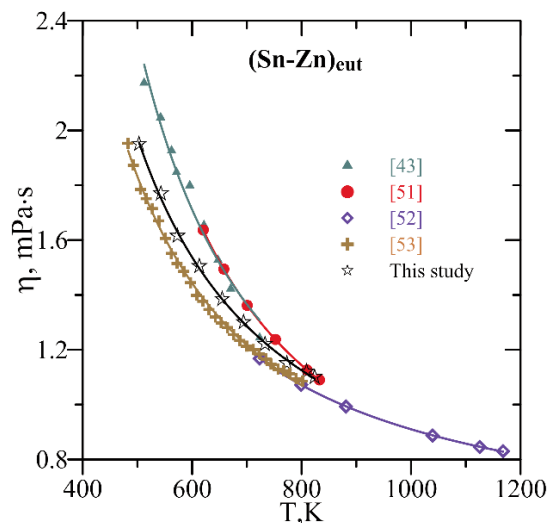


**Figure 10.** Comparison of temperature dependence of viscosity for Sn-Zn eutectic alloy measured in present work by the capillary method and those from the literature [43, 51-53]

Arrhenius equation shown in Table 3. As can be seen from this chart, the dynamic viscosity of the liquid alloy increases with the addition of indium, creating a peak. This peak partially coincides with the area of gamma phase existence. As the temperature increases, the viscosity peak disappears. This may suggest formation the In-Sn associates in the liquid.

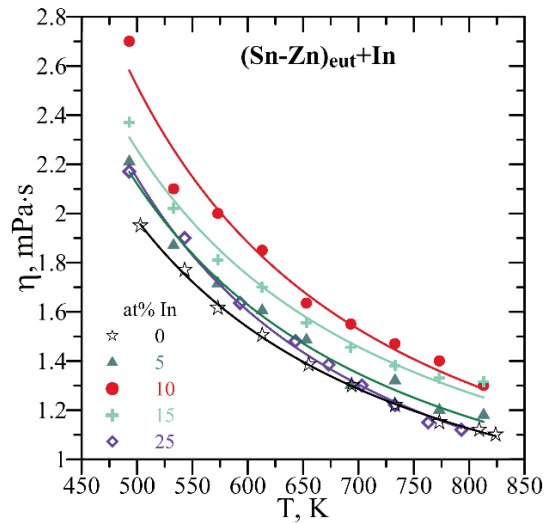


**Figure 11.** The temperature dependence of viscosity for  $(\text{Sn-Zn})_{\text{eut}} + \text{In}$  liquid alloys.

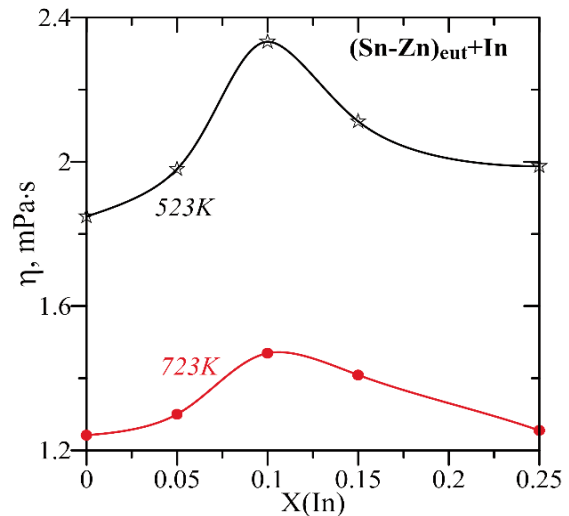


**Figure 12.** Isotherms of viscosity vs. concentration of indium for  $(\text{Sn-Zn})_{\text{eut}} + \text{In}$  alloys.

### 3.2 Wettability

The main parameters characterizing the wetting ability of solids with a liquid are the wetting angle and the magnitude and speed of spreading [34, 54]. Depending on the measurement conditions, these



values differ significantly. This is so because these are the result of many processes that are taking place at the interface. These processes are not fully understood or described. There is no simple answer what is driving force of the wetting process.

Spreading and wetting tests results of Sn – Zn – In alloys on copper pads presented in Figs. 13 and 14. Figure 13 shows that in the area of the existence of the gamma phase the wettability is improved. The spreading area increases and the contact angle decreases. However, the results indicate that wetting properties of this solder on copper pads do not depend on concentration of indium.

Lee and Shieu [ 55] studied the microstructure of the

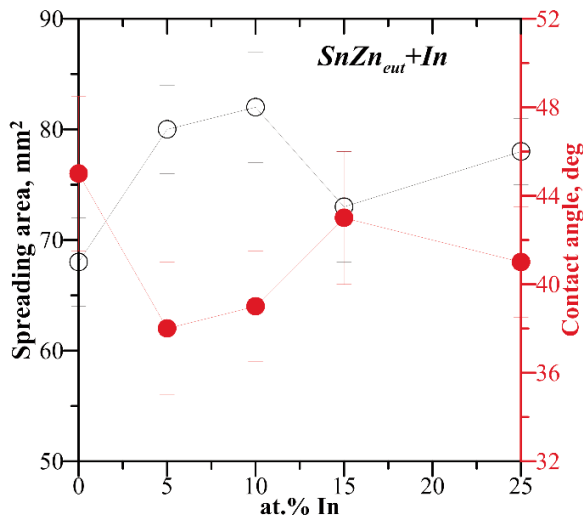


Figure 13. The results of the wetting tests in  $T=250C$  for 2 minutes.

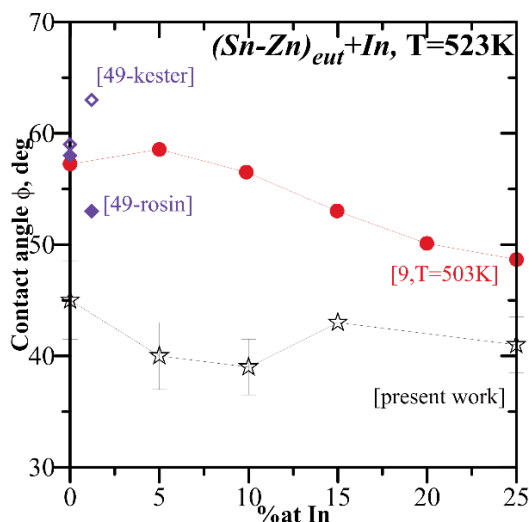


Figure 14. Comparison of contact angle  $\phi$  isotherms vs. concentration of indium for  $(Sn-Zn)_{eut} + In$  alloys measured in present work by the sessile drop method and those from the literature [9, 49] – meniscograph, [42] – sessile drop method.

Sn-15Zn/Cu interface, depending on temperature and the type of the resulting intermetallic compound. After wetting at 250 and 270 °C, grains of  $\epsilon-CuZn_4$  and  $\gamma-Cu_5Zn_8$  were formed, respectively. Figure 15 shows the microstructure of the solder joints of Sn-Zn-xIn/Cu obtained at 250 °C, after a wetting duration of 2 min. Starting from the pad, as in the previous [20, 26-32, 34, 55], from the side of solder there is  $\gamma-Cu_5Zn_8$ , and from the side of solder, there is a thin strip of  $\epsilon-CuZn_4$  phase. Fig. 16 illustrates the thickness of  $\epsilon-CuZn_4$  and  $\gamma-$

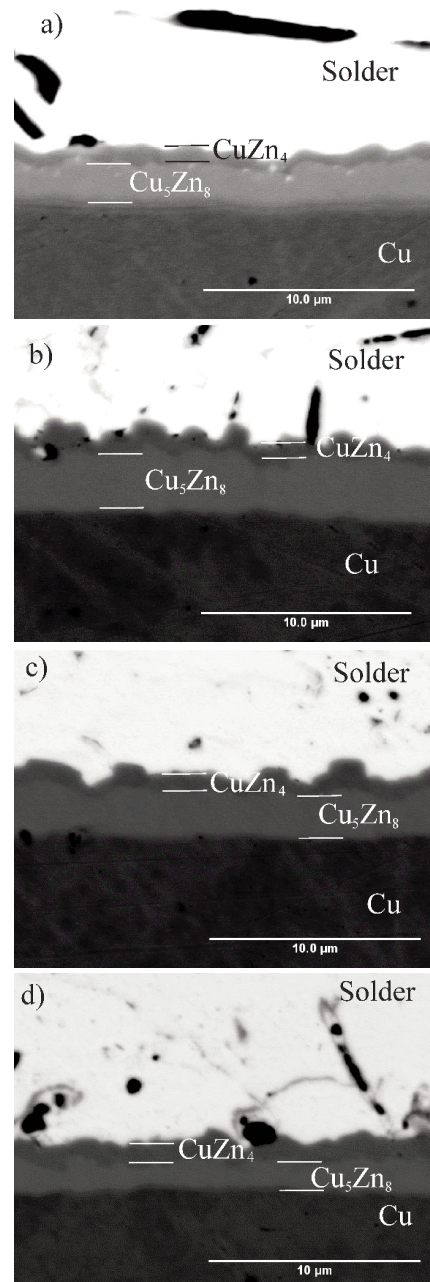


Figure 15. Microstructure and EDX analysis of Sn-Zn/Cu interface, after wetting for 3 min, in nitrogen at 250 C with ALU33 flux

$\text{Cu}_5\text{Zn}_8$  IMPs vs indium concentration. The layer thickness of the epsilon phase is practically constant for all concentrations of In. Whereas the addition of indium to the Sn-Zn eutectic alloy generally results in a reduction in the thickness of the gamma-layer. As with to the physicochemical properties, at the place of occurrence of the  $\gamma$ -In-Sn phase on the phase diagram (Fig.1), the maximum thickness of this layer also appears (Fig.15).

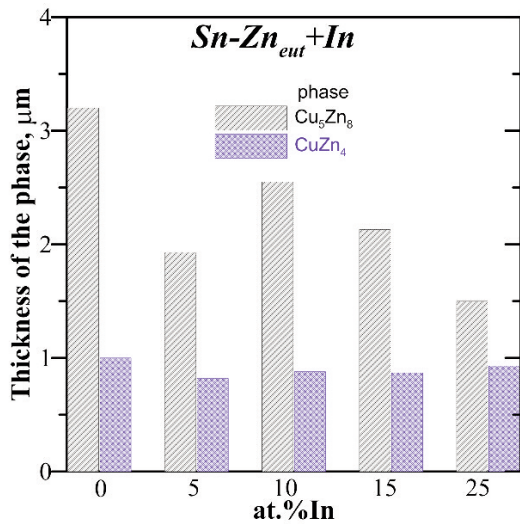


Figure 16. Thickness of intermetallic layers ( $\text{Cu}_5\text{Zn}_8$ ,  $\text{CuZn}_4$ ) at Solder/Cu interface at 250 °C, time-2min, solder –  $(\text{Sn-Zn})_{\text{eut}} + 5\% \text{In}$ ,  $(\text{Sn-Zn})_{\text{eut}} + 10\% \text{In}$ ,  $(\text{Sn-Zn})_{\text{eut}} + 15\% \text{In}$  and  $(\text{Sn-Zn})_{\text{eut}} + 25\% \text{In}$ .

#### 4. Discussion

The wetting process of solid substrates by liquid metals can be divided into two stages: the first involves physical adsorption and the second involves diffusion processes requiring energy activation. In the process of physical adsorption between the adsorbate and the adsorbent, the van der Waals interaction appears. The Van der Waals forces are weak, but with long range. At first, one-component phase A and B are in contact with each other, next which then form solid solutions A in B and B in A. Once the solutions are saturated, the formation of a new AxBy phase begins, it which creates a layer on boundary interface A and B. The new AxBy phase is not stoichiometric, has the character of a solid solution in which the maximum concentrations of component A occur at the boundary of component A and the maximum concentrations of component B at the boundary with component B.

The most important task of the flux is to purge the combined parts from oxides and other impurities. During this operation on the surface substrate there are places named as Langmuir active centers. Each center can absorb only one particle, that is, the

adsorbent is covered with a monomolecular layer. When the activation energy is relatively large, the diffusion of atoms begins. Sometimes in the soldering process occurs a so-called incubation time of the IMC layer. This “incubation time” is probably related to the attainment of the activation energy by the atoms adsorbed on the surface.

Wetting of metals by liquid metals is primarily related to the work of adhesion and cohesion. Adhesion work is a work that allows you to detach liquid from a solid surface area while simultaneously creating two new surfaces of the same size: liquid-gas and solid-gas (Fig.17).

Work cohesion –  $W_K = 2\sigma$  (4) [56], work adhesion –  $W_{ad} = \sigma(1 + \cos\phi) = 1/2 W_K(1 + \cos\phi)$  (5) [56].

Where  $\sigma$  – surface tension of liquid [mN/m],  $\phi$  – contact angle.

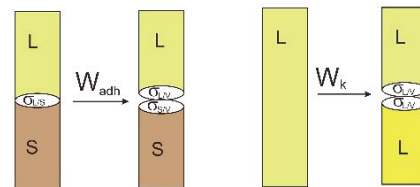


Figure 17. Work needed to overcome the forces of adhesion and cohesion. „S,V,L” – solid, gas, liquid

The spread of a non-reactive liquid on the surface of a solid is spontaneous. Its speed depends on the surface tension, interfacial tension, viscosity and density of the liquid.

In the case of spreading of metallic liquids on solid substrates there are other processes such as diffusion, dissolution and solidification. These processes go all the time, therefore there is no true equilibrium state in such systems. In this article, the wetting time was 2 minutes. We assume that after this time has been “frozen” the state of equilibrium. Therefore, we have calculated the work of adhesion and flow. Cohesion work  $W_K$  was calculated from formula (4), adhesion work  $W_{ad}$  from formula (5), spreading coefficient SC from formula (6), interfacial tension of solid/liquid  $\sigma_{SL}$  from Young-Dupre formula (7) [56]:

$$SC = \sigma_{SV} - \sigma - \sigma_{SL} = \sigma_{LV}(\cos\phi - 1) \quad (6)$$

$$\sigma_{SL} = \sigma_{SV} - \sigma \cos\phi \quad (7)$$

Where  $\sigma_{SV}$  – surface energy of solid Cu (1.825, J/m<sup>2</sup> [57]),  $\sigma_{SL}$  – interfacial tension of solid/liquid.

The value of spreading coefficient is negative for partial wetting state since the sum of surface tension and interfacial tensions is greater than the solid surface energy. Hence it is unfavourable to replace the solid / vapor interface via the solid / liquid interface.

Table 4 compares the physicochemical properties

**Table 4.** Comparison the physicochemical of Sn-Zn + xIn liquid solder with the wettability of the copper substrate by this solder.  $\delta$  – thickness of the IMC.

Solders	$\Delta V_M^{Ex}$	$\eta(523K)$	$E$	$W_K$	$W_{ad}$	$SC$	$\sigma_{SL}$	$\varphi$	$\delta$
(Sn-Zn) <sub>eut</sub>	0.155	1.85	6.231	1081	923	-158	1443	45	4.2
(Sn-Zn) <sub>eut</sub> +5%In	0.185	1.98	6.582	1077	951	-126	1413	40	2.75
(Sn-Zn) <sub>eut</sub> +10%In	0.27	2.33	7.256	1084	964	-121	1402	39	3.43
(Sn-Zn) <sub>eut</sub> +15%In	0.264	2.11	6.381	1078	933	-145	1431	43	3
(Sn-Zn) <sub>eut</sub> +25%In	0.139	1.99	7.232	1083	952	-133	1416	41	2.43

of Sn-Zn + xIn liquid solder (molar volume, viscosity and cohesion) with wettability values (adhesion, flow rate, interfacial tension, contact angle). The molar volume has been calculated from the experimental data of the density while the work of cohesion from the experimental surface tension data.

As previously described in the solder/Cu interface, a layer of intermetallic phases from the Cu-Zn system is formed. It can therefore be assumed, that the zinc atoms are adsorbed onto the surface of the copper at the first stage of the wetting process. That is, the size and the rate of reaction of the interface depend on the level of activity of these atoms.

Table 4 shows, that the addition of indium to the Sn-Zn eutectic alloy results in a reduction of IMC layer thickness from 4.2 to 2.43  $\mu\text{m}$ . It also improves the efficiency associated with the wettability (reduces contact angle, increases adhesion, and spreading coefficient S.C.). Thus we can suppose that the activity of Zn atoms in the liquid solder decreases with the addition of In in the solder. However, these changes are not directly proportional to the indium content. There are maxima and minima that correlate with the  $\gamma$  – Sn-In phase in the phase diagram.

Similar relationships were observed for physicochemical properties of liquid Sn-Zn-In alloys. The occurrence of maxima of the molar volume and the viscosity was noted. Only the surface tension was practically unchanged with the increase in the indium content. It can therefore be assumed, that interatomic interactions in liquid solutions have an influence not only on physicochemical properties but also on processes occurring during the wetting of metals substrates.

## 5. Conclusion

The measurements of density, surface tension and viscosity of Sn-Zn + xIn liquid solder were performed. It was shown that with increasing temperature, the density, viscosity and surface tension of the alloys tested decreases.

The addition of indium did not change the surface tension, but increased the viscosity and molar volume. It has also been observed that maxima and minima are

formed in the area of occurrence of  $\gamma$  – Sn-In on the phase diagram.

The measurements of wettability of Cu substrate by Sn-Zn eutectic-based alloys with 5, 10, 15 and 25 at.% of Indium were conducted by “sessile drop” method. Wetting process was studied at 250°C, in the presence of ALU33® flux, with wetting time of 2 minutes. The indium addition improves the solder wettability. The addition of indium has improved solder wettability, reducing the wettability angle from 45 to 39 degrees, and increasing adhesion from 923 to 964  $\text{Jm}^{-2}$ . The best effect has been achieved when the indium content in the solder was 10 at% .

The study of microstructure evolution of the interface between Sn-Zn-xIn alloys on Cu substrate has been performed with the “sessile” drop method. In the case of copper, substrate formation of intermetallic interlayers is observed. Two intermetallics can be distinguished at the interface, one  $\gamma$  –  $\text{Cu}_5\text{Zn}_8$  adjacent to the substrate, and the other  $\epsilon$  –  $\text{CuZn}_4$  adjacent to solder. The thickness of the intermetallic interlayers decreases during the indium addition. The smallest thickness IMC layer achieves for solder with 25% the indium additive (2.43 $\mu\text{m}$ ), the largest IMC layer thickness was formed solder with 10% the indium additive (3.43 $\mu\text{m}$ ).

## Acknowledgement

This work was financed within the framework of the project POIG.01.01.02-00-015/09 (Advanced materials and their production technologies, ZAMAT), co-funded by the European Regional Development Fund (ERDF).

## References

- [1] Directive 2002/96/WE Parlamentu Europejskiego z dnia 27 01 2003.
- [2] Directive 2003/108/WE Parlamentu Europejskiego z dnia 08 12 2003.
- [3] Directive 2008/35/WE Parlamentu Europejskiego z dnia 11 03 2008.
- [4] S. Vaynman, G. Ghosh, M.E. Fine, Mater. Trans., 45 (2004) 630-636.
- [5] J. Villain, W. Jilck, E. Schmitt, T. Qasim, Proceedings



- of the 2004 International IEEE Conference on the Asian Green Electronics, AGEC (IEEE Cat. No. 04EX769), (2004) 38-41.
- [6] Z. Moser, W. Gąsior, J. Pstruś, S. Książek, J. Electron. Mater., 31 (2002) 1225-1229.
- [7] L. Zhang, S. Xue, L. Gao, Z. Sheng, H. Ye, Z. Xiao, F. Zeng, Y. Chen, S. Yu, J. Mater. Sci., Mater. Electron. 21 (2010) 1-15.
- [8] G. Ren, I. J. Wilding, M. N. Collins, J. Alloys Compd. 665 (2016) 251-260.
- [9] 36.Ganesan S., Pecht M., Lead-free Electronics, Wiley-Interscience, (2006).
- [10] M. McCormack, S. Jin, J. Electron. Mater., 23 (1994) 635-640.
- [11] M. McCormack, S. Jin, J. Electron. Mater., 23 (1994) 715-720.
- [12] R.K. Shiue, L.W. Tsay, C.L. Lin, J.L. Ou, Microelectron. Reliab. 43 (2003) 453-463.
- [13] Hwang J.S., Lead-free Implementation and Production, A Manufacturing Guide, McGraw-Hill, 2005.
- [14] P. Sebo, P.Stefanik, Kovove Mater., 43, (2005), 202-209.
- [15] T.Takemoto, M.Miyazaki, Mater. Trans. 42, (2001) 745-750.
- [16] P. Fima, T. Gancarz, J. Pstrus, K. Bukat, J. Sitek, Sold. Surf. Mt. Techn., 24 (2012) 71-76.
- [17] U.S. Mohanty, K.L. Lin, Corros. Sci. 49 7 (2007) 2815-2831.
- [18] J.X. Jiang, J.E. Lee, K.S. Kim, K. Sukanuma, J. Alloys Compd. 462 (2008) 244-251.
- [19] X.J. Wang, Q.S. Zhu, B. Liu, N. Liu, F. J. Wang, J. Mater. Sci. Mater. Electron. 25(5) (2014) 2297-2304.
- [20] L. Zhang, L. Sun, Y.H. Guo, J. Mater. Sci. Mater. Electron. 25(3) (2014) 1209-1213.
- [21] Y. Xie, H. Schicketanz, A. Mikura, Ber. Bunsenges. Phys. Chem., 102 (1998) 1334- 1339.
- [22] Vaynman S., Fine M.E., Scripta Mater., 41, (1999), 1269.
- [23] Y.Cui, X.J. Liu, I. Ohnuma, R. Kainuma, H. Ohtani, J. Alloys Compd., 320 (2001) 234.
- [24] Z. Moser, Z. Metallkd. 65 (1974) 106-111.
- [25] C.K. Behera, A. Sonaye, Thermochimica Acta 568 (2013) 196-203.
- [26] X. Chen, A.Hu, M. Li, D. Ma, J. Alloys Compd., 460 1-2 ( 2008) 478-484.
- [27] G. Ren, M. N. Collins, Mater. Des. 119 (2017) 133-140.
- [28] P. Fima, T. Gancarz, J. Pstruś, A. Sypień: J. Mater. Eng. Perform., 5 21 (2012) 595-598.
- [29] M.L. Huang, Z.J. Zhang, N. Zhao, Q. Zhou, Scr. Mater. 68(11) (2013) 853-856.
- [30] Y. Yao, X. Feng, Z. Jian, F. Zhanying, C. Xu, J. Mater. Eng. Perform, 24 (2015) 2908-2916.
- [31] F. Xing, J. Yao, J. Liang, X. Qiu, J. Alloys Compd., 649 (2015) 1053-1059.
- [32] H. Ye, S.B. Xue, J.D. Luo, Y. Li, Mater. Des. 46 (2013) 816-823.
- [33] N.F. Dorsey, J. Wash. Acad. Sci., 18 (1928) 505-509.
- [34] J. Pstruś, P. Fima, T. Gancarz, J. Mater. Eng. Perform., 5 21 (2012) 606-613.
- [35] T.Gancarz, Z. Moser, W. Gąsior, J. Pstruś, H.Henein, Int. J. Thermophys., 30 (2011) 1210-1233.
- [36] W. Gąsior, Z. Moser, J. Pstrus, J. Phase Equilib. Diffus., 19 (1998) 234-238.
- [37] W. Gąsior, Z. Moser, J. Pstruś, J. Phase Equilib. Diffus., 24 (6) (2003) 504-510.
- [38] B.J. Lee, C.S. Oh, J.H. Shin, Journal of Electronic Materials 25 (1996) 983.
- [39] C.C. Jain, S.S. Wang, K.W. Huang, T.H. Chuang, J. Mater. Eng. Perform., 18 (2009) 211-215.
- [40] H.-M. Wu, F.-C. Wu, T.-H. Chuang, J. Electron. Mater., 34 (2005) 1385-1390.
- [41] T. H. Chuang, K.W. Huang, and W.H. Lin, J. Electron. Mater., 33 (2004) 374-380.
- [42] J. Pstruś, Physico-Chemical Properties of New Solder Alloys on Example of Sn-Zn-In System, Ph.D. Thesis, Krakow, 2008.
- [43] T. Gancarz, J. Pstruś, W. Gąsior, H. Henein, J. Electron. Mater., 42 2 (2013) 288-293.
- [44] D. Yagodin, V. Sidorov, D. Janickovic, P. Svec, J. Non-Cryst. Solids, 358 (2012) 2935-2937.
- [45] K.Bukat, Z.Moser, J.Sitek, W.Gąsior, M.Kościelski, J.Pstruś, Sold. Surf. Mt. Techn., 22, (2010), 10-16.
- [46] Z. Moser, W. Gąsior, J. Pstruś, I. Kaban, W. Hoyer, Int. J. Thermophys., 30 (2009) 1811-1822.
- [47] J. Pstrus, Z. Moser, W. Gąsior, Applied Surface Science 257 (2011) 3867.
- [48] J. Pigozin, R. Diefel, Chemiczeskaja tiermodinamika, Nowosibirsk 1966. (in Russian)
- [49] M.E. Loomans, S. Vaynman, G. Ghosh, M.E. Fine, J. Elec. Mat. 23 (8) (1994)741-748.
- [50] W.Gąsior, Z. Moser, J.Pstruś, M.Kucharski., Arch. Metall. Mater., 46 (1) (2001) 23-32.
- [51] T. Sato and S. Munakata, Bull. Res. Inst. Miner. Dress. Metall. 11 (1955) 183.
- [52] A.F. Crawley, Metall. Trans., 3 (1972) 157.
- [53] Yu. Plevachuk, V. Sklyarchuk, P. Svec Sr, P. Svec, D. Janickovic, E. Illekova, A. Yakymovych, J. Mater. Sci: Mater. Electron., 28 (2017) 750-759.
- [54] D.R. Frear, W.B. Jones, K.R.Kinsman, A TMS Publication; (1991)1-104.
- [55] C.S. Lee and F.S. Shieu, J. Electron. Mater., 35 (2006) 1660-1666.
- [56] Bartell F.E., Osterhof H.J., Koloid Symposium Momograph, New York, 1928, The Chemical Catalog Co., Ins, 113.
- [57] W.R. Tyson, W.A. Miller, Surf. Sci., 62 (1977) 267.

